ACS APPLIED MATERIALS & INTERFACES

Research Article

www.acsami.org

Constructing Higher-Order DNA Nanoarchitectures with Highly Purified DNA Nanocages

Shu Xing,[†,‡] Dawei Jiang,[†,‡] Fan Li,[‡] Jiang Li,[‡] Qian Li,[‡] Qing Huang,[‡] Linjie Guo,[‡] Jiaoyun Xia,[‡,§] Jiye Shi,[‡] Chunhai Fan,[‡] Lan Zhang,*[,‡] and Lihua Wang*[,‡]

[‡]Division of Physical Biology & Bioimaging Center, Shanghai Synchrotron Radiation Facility, Shanghai Institute of Applied Physics, Chinese Academy of Sciences, Shanghai 201800, China

[§]College of Chemistry and Biological Engineering, Changsha University of Science and Technology, Changsha 410004, China

Supporting Information

ABSTRACT: DNA nanostructures have attracted great attention due to their precisely controllable geometry and great potential in various areas including bottom-up self-assembly. However, construction of higher-order DNA nanoarchitectures with individual DNA nanostructures is often hampered with the purity and quantity of these "bricks". Here, we introduced size exclusion chromatography (SEC) to prepare highly purified tetrahedral DNA nanocages in large scale and demonstrated that precise quantification of DNA nanocages was the key to the formation of higher-order DNA nanoarchitectures. We successfully purified a series of DNA nanocages with different sizes, including seven DNA tetrahedra with different edge lengths (7, 10, 13, 17, 20, 26, 30 bp) and one trigonal bipyramid with a 20-bp edge. These highly purified and aggregation-free DNA nanocages could be self-assembled into higher-order DNA nanoarchitectures with extraordinarily high yields (98% for dimer and 95% for trimer). As a comparison, unpurified DNA nanocages resulted in low yield of 14% for dimer and 12% for trimer, respectively. AFM images cleraly presented the characteristic structure of monomer, dimer and trimer, impling the purified DNA nanocages well-formed the designed nanoarchitectures. Therefore, we have demonstrated that highly purified DNA nanocages are excellent "bricks" for DNA nanotechnology and show great potential in various applications of DNA nanomaterials.

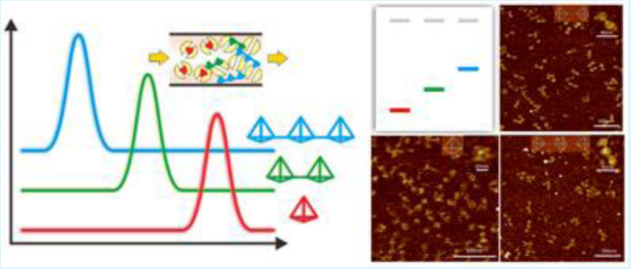

KEYWORDS: *DNA tetrahedron, size exclusion chromatography, purification, quantification, highly ordered DNA nanoarchitectures*

1. INTRODUCTION

In the past decade, DNA architectures have attracted great attention for their precisely controllable geometry and great potential in various areas.[1−3] Compared to inorganic nanomaterials, bottom-up-fabricated DNA nanostructures through Watson−Crick base pairing have unprecedented advantages including precise controllability, sequence specificity, chemical reactivity, and spatial addressability. Up to now, 2D and 3D DNA nanostructures with tunable size and shape, mechanical flexibility, and diverse surface modification have been achieved.[3−7] In addition, the heteroelemental organization of DNA nanostructures with various materials, including proteins,[8] peptides,[9] virus capsids,[10] nanoparticles,[11−16] and carbon nanotubes,[17] endows them with myriad possibilities for designing various probes and drugs to locate specific positions and access desired functions in vivo.

However, it remains a challenge to prepare higher-order DNA nanoarchitectures with large size in large scale, which is important for realizing complicated functions.[1,2] Although it is possible to use DNA origami to fold large nanoarchitectures,[18−21] the mechanical fragility and synthetic difficulty of ssDNA scaffold and the purity of DNA nanoarchitectures often lead to high cost and low yield. Another approach is to assemble preformed small structures (including small tiles and even origamis), which called "DNA bricks", into supramolecular assemblies of higher-order DNA nanoarchitectures.[22,23] In this case, it is essential to precisely quantify these small "bricks" for high-yield assembly of higher-order architectures. Despite continued efforts have been taken to optimize the structural design and assembly conditions, the yields of most delicate bricks are relatively low.[24] Some unwanted byproducts, including misfolded structures, aggregates, and ssDNAs, often interfere with the assembly of higher-order DNA nanoarchitectures.

As an excellent example, tetrahedral DNA nanocages are a type of bricks to construct large nanoarchitectures. These tetrahedra are usually composed of several designed ssDNA strands and their sizes can be easily tuned by changing the edge length. Also, they can be precisely modified at specific sites and conjugated with various kinds of molecules through appropriate

Received: August 19, 2014
Accepted: October 27, 2014
Published: October 27, 2014

DOI: 10.1021/am505592e
ACS Appl. Mater. Interfaces 2015, 7, 13174−13179

Scheme 1. (a) Construction of Higher-Order DNA Nanoarchitectures; (b) SEC Purification of Various DNA Nanocages and Nanoarchitectures

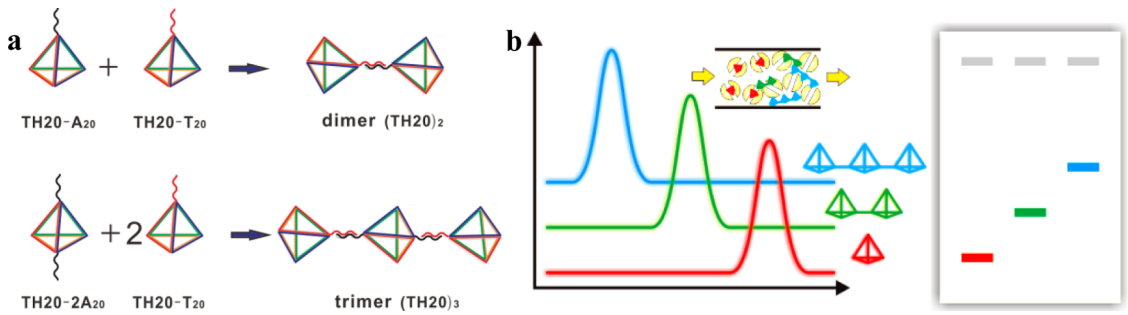

conjugation chemistry. By virtue of these advantages, DNA tetrahedra have proven to be a type of excellent biosensing platforms to control the probe density and improve signal transduction of a range of biomolecules.[25−29] More recently, DNA tetrahedra were found to be excellent carrier to transport cargo molecules into live cells for imaging and therapy.[4,8,28,30−34]

In this work, a series of DNA tetrahedra with different sizes and modifications, including seven DNA tetrahedra with different edge lengths (7−30) and a DNA trigonal bipyramid, were synthesized through self-assembly. These nanocages were extensively purified with size exclusion chromatography (SEC) to obtain aggregates-free monomers, which could be precisely quantified. These highly purified DNA nanocages were used to construct higher-order DNA nanoarchitectures with extraordinarily high yields (Scheme 1).

2. EXPERIMENTAL SECTION

2.1. Materials. DNA oligonucleotides were purchased from InvitrogenTM (Shanghai, China). Amicon filters were purchased from Millipore (Billerica, MA, USA). GelRed DNA gel stain solution was purchased from Biotium (USA). Tris (hydroxymethyle) aminomethane (Tris Base) was purchased from Aladdin (Shanghai, China, ≥99.9%). All other reagents were purchased from Sinopharm Chemical Reagent Co. Ltd. (Shanghai, China). All oligonucleotide sequences were listed in the Supporting Information. SEC data were obtained using a Waters HPLC system with an in-line degasser, a binary HPLC pump (Waters 1525) and a photodiode array detector (Waters 2998). AFM was performed on a Multimode 8 atomic force microscope (Bruker, USA).

2.2. Self-Assembly of DNA Cages. Assembly of DNA cages was accomplished in a single annealing step as reported previously.[29] TM-1 buffer (20 mM Tris-HCl, 50 mM $MgCl_2$, pH 8.0) was used for the assembly of TH7, TH10, TH13 and TH17, and TM-2 buffer (10 mM Tris-HCl, 5 mM $MgCl_2$, pH 8.0) was used for TH20, TH20-A_{20}, TH20-T_{20}, TH20−$2A_{20}$, TH26, TH30 and TB20. All tetrahedra with different edge lengths were synthesized by mixing equimolar quantities (1 μM) of oligonucleotides in hybridization buffer (TM-1/TM-2 buffer), heating to 95 °C for 5 min, then rapidly cooling to 4 °C in a PCR machine (Applied Biosystems Veriti 96 well Thermal Cycler). TB20 was assembled by mixing six strands in equimolar amounts (0.17 μM) in TM-2 buffer, annealing in boiled water bath and then cooling to room temperature over 30 min. All cages were characterized by 8% ∼ 10% native polyacrylamide gel electrophoresis (PAGE) and yields were semiquantified using ImageJ software.

2.3. Purification of DNA Cages by SEC. A SEC column (Phenomenex BioSec-SEC-S2000, 300*7.8 mm) was used and all chromatograms were recorded at 260 nm. A typical SEC mobile phase was 30 mM Tris-HCl, pH 7.4, 450 mM NaCl. 50−500 μL of as-prepared DNA cages were loaded and purified at a flow rate of 0.6 mL/min with isocratic elution. Other purification conditions for various cages were listed in Table S2 in the Supporting Information.

2.4. Calculation of SEC Separation Resolution. Resolution (R) was calculated using an equation: $R = 2(t_{R2} - t_{R1})/(W1 + W2)$, where t_{R1} and t_{R2} are the retention time of two adjacent peaks in SEC chromatograms, and $W1$ and $W2$ are their corresponding peak widths.

2.5. PAGE Analysis of SEC Purified DNA Nanocages. Peak fractions collected from SEC were concentrated into desired volume at <3000 g for 5−20 min using Amicon Ultra-0.5 mL centrifugal filters (MWCO 30 kDa) before PAGE analysis. An 8% gel was used for TH17, TH20, TH26, TH30, TH20-T_{20} (A_{20}, $2A_{20}$) and TB20, whereas 10% was used for TH7, TH10, and TH13. PAGE was performed in 1× TBE buffer (or 1× TAE) including 12.5 mM $MgAc_2$ at 4 °C for 2−3 h, and DNA was stained with GelRed for 15−30 min for further analysis on a chemiluminescence imaging system (G:Box Chemi-XL).

2.6. Stability of Purified DNA Nanocages. The purified TH20 was stored at 4 °C in mobile phase buffer. The integrity of structure was investigated using SEC and PAGE after 1, 3, 7, 15, and 30 days.

2.7. T_m Analysis and Quantification of Three DNA Tetrahedra. Melting curves of three SEC purified DNA tetrahedra (TH17, TH20, and TH26) were recorded using UV−visible Spectrophotometer (Cary100 Bio, USA). The sample solutions are heated from 25 to 100 °C at a constant rate of 1 °C/min.

2.8. "Bottom-up" Construction of Higher-Order DNA Nanoarchitectures. For dimer preparation, unpurified or SEC purified TH20-T_{20} and TH20-A_{20} were mixed in a molar ratio of 1:1 in mobile phase buffer, and the reaction solution was gently mixed for 15 min at room temperature. For trimer, TH20-T_{20} and TH20-$2A_{20}$ were mixed in a molar ratio of 2:1. The reaction products were characterized using SEC and PAGE (6%, 100 V for 2h at 4 °C).

2.9. Characterization of Different DNA Nanoarchitectures Using AFM. Freshly cleaved mica surface was modified with 0.5% APTES for 2 min, and washed off by Milli Q water (18 MΩ·cm) and dried by compressed air. DNA nanostrucutures, diluted to 10 nM in TM-2 buffer in 10 μL, were spotted onto mica surface and incubated for 5 min to allow the sample to absorb onto the substrate. After that, additional TM-2 buffer was added to a total volume of 40 μL, and the sample was scanned using an SNL-10 (Veeco Inc., USA) with supersharp tips of 2−3 nm radius.

3. RESULTS

3.1. Preparation and Characterization of DNA Nanocages and Derivatives. In this work, eight DNA cages, i.e. seven tetrahedra and one trigonal bipyramid, were investigated for developing purification methods. Seven tetrahedra with different lengths of edge DNA (7, 10, 13, 17,[35] 20,[29] 26,[36] and 30 bp[37]) were prepared through self-assembly of several ssDNAs, and correspondingly were named as TH7, TH10, TH13, TH17, TH20, TH26, and TH30, respectively. A similar hollow structure, trigonal bipyramid with 20 bp-edge, was synthesized with six ssDNAs and named as TB20.[38] All these cages were characterized by PAGE analysis, with multibands indicating products formed in the assembly process (Figure 1a). Besides the desired well-folded monomer,

DOI: 10.1021/am505592e
ACS Appl. Mater. Interfaces 2015, 7, 13174−13179

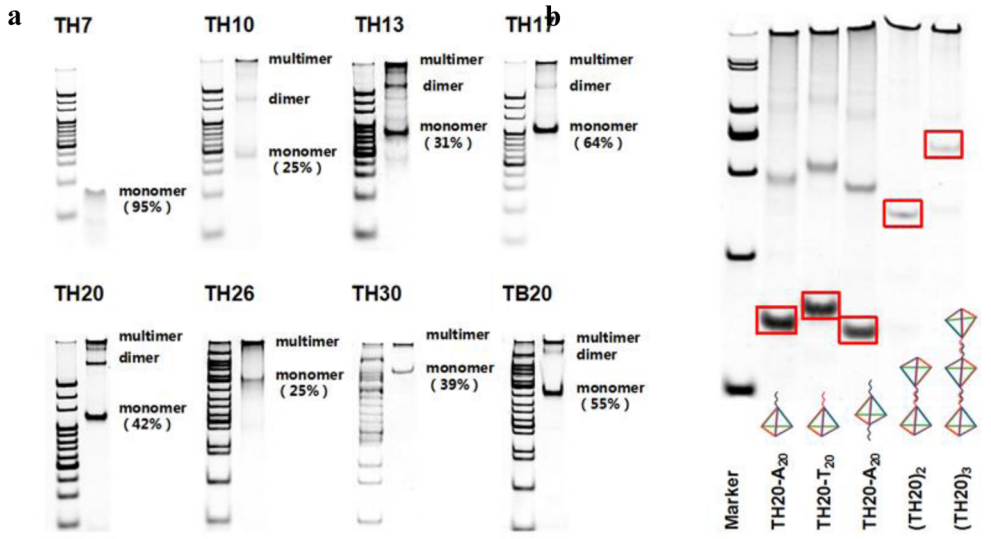

Figure 1. PAGE analysis of (a) eight DNA nanocages and (b) dimer and trimer prepared with raw TH20 products. M: marker DNA with 20bp Ladder.

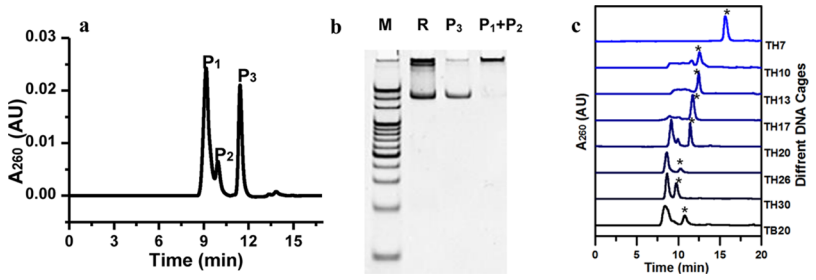

Figure 2. (a) Typical SEC chromatogram of TH20 cage. (b) 10% PAGE analysis of raw products (R), P_1, P_2, and P_3 fractions. (c) SEC spectra of different DNA cages with the desired monomer star-marked.

some aggregates and incomplete structures were formed as side products, and the yields of most DNA nanocages were estimated in the range of 25−64% while TH7 of 95%.

TH20 was selected as a model to investigate effect of purity on construction of higher-order DNA nanoarchitectures. S1-A_{20} and S1-T_{20} were used to fabricate single A_{20}- and T_{20}-overhung TH20 (TH20-A_{20}, TH20-T_{20}), which consequently form a dimer of $(TH20)_2$ through hybridization of A_{20} with T_{20}. The trimer of TH20, $(TH20)_3$, was prepared based on a similar design, in which a TH20 with two A_{20} arm strands (TH20−$2A_{20}$) and two TH20-T_{20} units were used (Scheme 1a). On the basis of PAGE analysis, yields of $(TH20)_2$ and $(TH20)_3$ were 14% and 12% (Figure 1b), respectively. The low yields and low purity of these DNA tetrahedra can not satisfy their application as "bricks" for constructing advanced nanoarchitectures.

3.2. SEC Purification of DNA Cages. On the basis of the size differences of the components in TH20 products, SEC was selected to isolate the monomer. A SEC column packed with porous particles of 14.5 nm diameter, larger than all DNA cages (in a range of 2.9−12.5 nm, see Table S1 in the Supporting Information) was employed. The chromatogram implied three components formed during assembly process, and the rentention time (t_R) of each component was 9.2, 9.9, and 11.4 min, respectively (Figure 2a). All peak fractions were collected and further analyzed by PAGE (Figure 2b). Component P_3 was identified as tetrahedron monomer, whereas P_1 and P_2 were aggregates. The separation efficiency of SEC was evaluated by separation resolution (R). The R was calculated as 2.8 for TH20, larger than 8σ-separation of 2, indicating that monomer was completely separated from aggregates.

Worthy of noting, the SEC purification was easily influenced by several factors, e.g. ion strength and the flow rate, which were optimized to achieve the best resolution (Figure S1 and Table S2 in the Supporting Information) in this work. With the optimized separation conditions, all DNA cages, including seven DNA tetrahedra with edges of 7, 10, 13, 17, 20, 26, 30 bp and one bipyramid cage with 20 bp-edge, were well purified. Figure 2c demonstrated that all cages could be isolated from their aggregates, and the resolution of all cages was in the range of 1−3 (see Table S1 in the Supporting Information).

3.3. Recovery, Storage, And Quantification of TH20. 500 pmol (prepared in 1 μM and 500 μL per batch, about 45 μg) of TH20 can be loaded on analytical column and isolated within 15 min per batch, therefore, we can easily recover large quantity of TH20 in mg level through repeating the SEC purification procedures. Compared to purification with PAGE (<1 μg, complicated recovery procedure taking several hours), the SEC procedure is simpler and more efficient.

SEC purified TH20 (in mobile phase buffer) were stored at 4 °C for 1, 3, 5, 7, 15, and 30 days and their integrity was characterized by SEC (Figure 3a) and PAGE (see Figure S2 in the Supporting Information). The results indicated degradation or reaggregation of monomer did not occur.

For precise quantification of DNA tetrahedron, we chose TH17, TH20, and TH26 to study their hyperchromic effect and calculate their molar extinction coefficient (ε). The SEC

DOI: 10.1021/am505592e
ACS Appl. Mater. Interfaces 2015, 7, 13174−13179

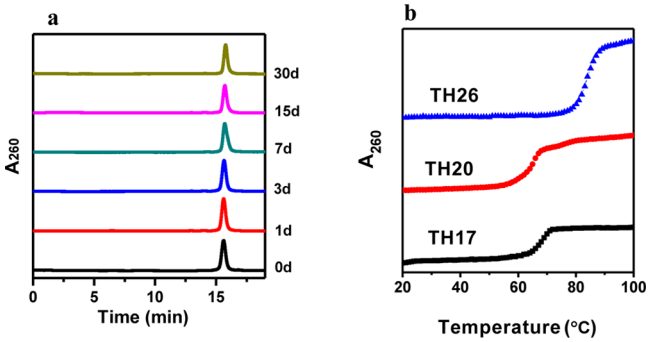

Figure 3. (a) Chromatograms of SEC purified TH20 in mobile phase buffer stored at 4 °C; (b) melting curves of SEC purified TH17, TH20, and TH26.

purified tetrahedral monomers were melted into ssDNAs by increasing temperature (Figure 3b). The T_m and ε of each tetrahedron are listed in Table 1 and the results indicated

Table 1. Some Characteristics of Three DNA Tetrahedra

	TH17	TH20	TH26
T_m (°C)	69	65, 75	84
A_{260}@95 °C/A_{260}@25 °C	1.31	1.28	1.29
ε_{TH} ($\times 10^6$ L mol^{-1} cm^{-1})	1.87	2.18	2.82

bigger tetrahedra have higher Tm as expected. The A_{260} of ssDNAs (A_{260}@95 °C) was about 1.3 times of that in tetrahedron form (A_{260}@25 °C), and this hyperchromic effect of tetrahedron was similar to that of dsDNA (generally 1.2−1.4 times). Therefore, we can easily quantify the concentration of tetrahedron through the Beer's Law ($A_{260} = \varepsilon bC$) and the characterized ε (about 0.77 of ε_{ssDNAs}).

3.4. Construction of Higher-Order DNA Nanoarchitectures with Purified TH20 Derivatives. Unpurified and SEC purified TH20 derivatives were used to construct large and complex nanoarchitectures, respectively, and the products were analyzed using SEC and PAGE (Figure 4). The yields of higher-order DNA nanoarchitectures using unpurified products of TH20 derivatives (14% for dimer and 12% for trimer, Figure 4a) were much lower than using the purified ones (98% for dimer and 95% for trimer, Figure 4b, c), which clearly indicated the dramatic negative effect of misfolded structures on the formation of desired DNA nanoarchitectures. The purified DNA architectures were then characterized using AFM, and the TH20 monomer, dimer and trimer were clearly characterized (Figure 4d-f). The structure of TH20 was uniform in monomer form after HPLC purification, and no aggregates appeared in the visual field (Figure 4d). The inset view shown the high resolution imaging of single monomer, and the size was 11.7 nm in length (see Figure S3a in the Supporting Information). The size was larger than that of the designed one (6.8 nm) because of the broadening effect arising from the AFM tips. The dimer in Figure 4e inset was estimated as 39.5 nm (see Figure S3b in the Supporting Information), and the trimer in Figure 4f was 53.1 nm (see Figure S3c in the Supporting Information). Significantly, the clear presentation of higher-order DNA architectures in visual form supported the high purity of them, and most of them existed in the designed forms. Interestingly, the oritention of TH20 in dimer and trimer was various, and they connected each other with uncertain perspective and formed various line and curves. This phenomenon might be explained by the relative flexibility of arm structure between TH20.

4. DISCUSSION

The well-designed DNA tetrahedron has been considered as good "bricks" for fabrication of higher-order and multifunctional 3D nanoarchitectures.[39] During its single-step preparation, unwanted byproducts including misfolded structures,

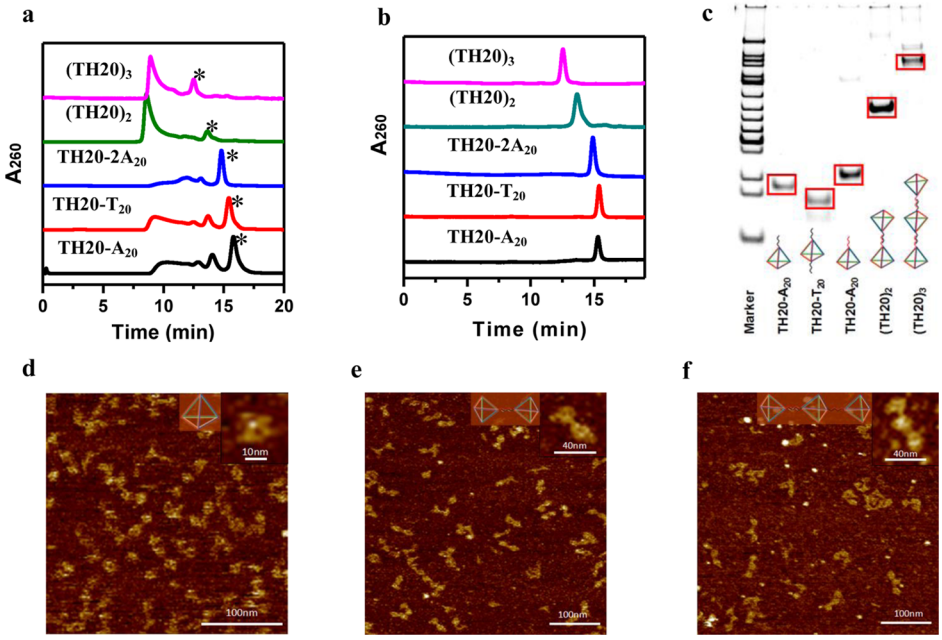

Figure 4. SEC chromatograms of TH20-A_{20}, TH20-T_{20}, TH20-$2A_{20}$, dimer, and trimer prepared with (a) unpurified DNA tetrahedra (the desired products were star-marked) and (b) SEC purified monomers; (c) corresponding PAGE results. The purified (d) monomer, (e) dimer, and (f) trimer were characterized using AFM, respectively, inset was the responding single DNA nanostructrue with high resolution.

DOI: 10.1021/am505592e
ACS Appl. Mater. Interfaces 2015, 7, 13174−13179

aggregates, and ssDNAs usually formed and coexisted with the desired monomers of DNA tetrahedron.

PAGE and agarose gel electrophoresis have been widely used for purification of DNA nanostructures, and PAGE is considered as a good approach to differentiate monomers from other impurities because of the high resolution. However, several disadvantages limit its application in large-sized DNA nanostructures. First, PAGE only provides semiquantification while a precise-quantification usually plays dominant role in fabrication of DNA nanoarchitectures. Second, most of PAGE photograph suffers from the remaining components in the loading wells, which will occur for any sample with unclear reason even for various markers. The disturbance confuses the researchers to make a correct judgment for all components and results in unfaithful quantification. Third, the DNA nanostructures risks the reaggregation and (or) degradation in identification and recovery process, which has been found in almost all PAGE data (Figures 1, 2b, 4c). This phenomenon may attribute to the electrophoresis buffer (1× TBE buffer or 1× TAE with 12.5 mM $MgAc_2$), the temperature increase along with the long period of electrophoresis, and other ignorance factors. Fourth, the recovery process is tedious and the recovery efficiency is low. A whole PAGE purification process usually takes several hours, including extraction, centrifugation, desalting and concentration processes. Due to limited loading quantity on gel (generally in 20 μL per hole) and limited binding capacity of extraction kit (~10 μg), the recovery efficiency for large DNA nanoarchitectures (less than 30%, data not shown) is low. Moreover, by using gel extraction kits, a heating treatment is commonly needed for accelerating dissolution of DNA from gel, which is not favored because DNA cages will be destroyed under high temperature.

To conveniently prepare pure DNA "bricks" in large scale, we required a more efficient purification method, together with a precise quantification procedure. Purification of DNA cages with PAGE and SEC were evaluated and the results were compared with each other. The separation resolution (R) of both methods could meet the requirement of getting pure monomers. However, SEC is superior to PAGE, with convenient and efficient recovery process and simple storage.

Generally, DNA cages were prepared with 500 μL volume and 1 μM concentration per batch, which could be loaded on the analytical column using a 500 μL sample loop. 500 pmol (about 45 μg) samples could be prepared per batch, which was much efficient than PAGE (<1 μg). No complicated post-treatment process was needed for SEC, and the collected products could be easily stored in eluent buffer at 4 °C for 30 days without degradation and reaggregation.

Furthermore, SEC-purified DNA tetrahedron monomers could be precisely quantified in eluent buffer based on the hyperchromic effect of DNA cages similar to dsDNA. A_{260} for TH20 increased about 30% after melting into ssDNAs, which meant the ε of TH20 was about 0.77 times of all ssDNAs in DNA tetrahedron. This method was considered to be general for quantifying different pure DNA nanostructures. In short, the efficient purification and precise quantification of DNA nanocages greatly contributed to the formation of higher-order DNA nanoarchitectures, with the significantly diminished formation of byproducts rising from the misfolded structures.

5. CONCLUSION

In this work, we have established a SEC method for efficient purification of rigid DNA tetrahedra, and the desired monomers were easily isolated from the aggregates and other byproducts. The purified DNA tetrahedra can be easily recovered in large scale (~45 μg per batch) with high purity (~95%), and then conveniently restored in eluent buffer at 4 °C for 30 days without degradation and reaggregation. We also precisely quantified the concentration of DNA tetrahedron and provide a characterized ε of DNA tetrahedron (0.77 times εssDNAs). "Bottom-up" construction of high-order DNA nanoarchitectures using ssDNA-overhang DNA tetrahedron is investigated, and the highly purified and precisely quantified DNA cages provided much higher yields (98% for dimer and 95% for trimer) in comparison with the unpurified ones (14% for dimer and 12% for trimer). AFM images cleraly presented the characteristic structure of monomer, dimer and trimer, impling the purified TH20 well formed the designed nanoarchitectures. This work provides an efficient way for preparing high quality DNA "bricks" to assembly higher-order 3D DNA nanoarchitecture, which exhibit great potential for application in biology and clinic medicine.

■ ASSOCIATED CONTENT

Supporting Information

Oligonucleotide sequences of these DNA nanocages, isocratic elution purification of DNA cages by SEC, some characters of SEC purification of DNA nanocages, the optimization of SEC for separation of TH20 and structural stability of purified TH20 in mobile phase at 4 °C. This material is available free of charge via the Internet at http://pubs.acs.org.

■ AUTHOR INFORMATION

Corresponding Authors

*E-mail: wanglihua@sinap.ac.cn.
*E-mail: zhanglan@sinap.ac.cn.

Author Contributions

†S.X. and D.J. contributed equally to this report

Funding

We thank the National Natural Science Foundation of China (21227804, 21390414, and 31371015), the National Basic Research Program of China (973 program, 2013CB932803) and the Youth Innovation Promotion Association, CAS for financial support.

Notes

The authors declare no competing financial interest.

■ REFERENCES

(1) Pinheiro, A. V.; Han, D.; Shih, W. M.; Yan, H. Challenges and Opportunities for Structural DNA Nanotechnology. *Nat. Nanotechnol.* **2011**, *6*, 763−772.

(2) Lan, X.; Wang, Q. B. DNA-Programmed Self-Assembly of Photonic Nanoarchitectures. *NPG Asia Mater.* **2014**, *6*, e97.

(3) Ke, Y. G. Designer Three-Dimensional DNA Architectures. *Curr. Opin. Struct. Biol.* **2014**, *27*, 122−128.

(4) Nangreave, J.; Han, D.; Liu, Y.; Yan, H. DNA Origami: A History and Current Perspective. *Curr. Opin. Chem. Biol.* **2010**, *14*, 608−615.

(5) Saccà, B.; Niemeyer, C. M. DNA Origami: The Art of Folding DNA. *Angew. Chem., Int. Ed.* **2012**, *51*, 58−66.

(6) Lin, C. X.; Jungmann, R.; Leifer, A. M.; Li, C.; Levner, D.; Church, G. M.; Shih, W. M.; Yin, P. Submicrometre Geometrically Encoded Fluorescent Barcodes Self-Assembled from DNA. *Nat. Chem.* **2012**, *4*, 832−839.

(7) Chen, Z.; Lan, X.; Wang, Q. B. DNA Origami Directed Large-Scale Fabrication of Nanostructures Resembling Room Temperature Single-Electron Transistors. *Small* **2013**, *9*, 3567−3571.

DOI: 10.1021/am505592e
ACS Appl. Mater. Interfaces 2015, 7, 13174−13179

(8) Erben, C. M.; Goodman, R. P.; Turberfield, A. J. Single-Molecule Protein Encapsulation in A Rigid DNA Cage. *Angew. Chem., Int. Ed.* **2006**, *45*, 7417−7421.
(9) Williams, B. A. R. Self-assembled Peptide Nanoarrays: An Approach to Studying Protein-Protein Interactions. *Angew. Chem., Int. Ed.* **2007**, *46*, 3051−3054.
(10) Stephanopoulos, N. Immobilization and One-Dimensional Arrangement of Virus Capsids with Nanoscale Precision Using DNA Origami. *Nano Lett.* **2010**, *10*, 2714−2720.
(11) Zhao, Z.; Lacovetty, E. L.; Liu, Y.; Yan, H. Encapsulation of Gold Nanoparticles in A DNA Origami Cage. *Angew. Chem., Int. Ed.* **2011**, *50*, 2041−2044.
(12) Nykypanchuk, D.; Maye, M. M.; van der Lelie, D.; Gang, O. DNA-Guided Crystallization of Colloidal Nanoparticles. *Nature* **2008**, *451*, 549−552.
(13) Lan, X.; Chen, Z.; Liu, B.-J.; Ren, B.; Henzie, J.; Wang, Q. B. DNA-Directed Gold Nanodimers with Tunable Sizes and Interparticle Distances and Their Surface Plasmonic Properties. *Small* **2013**, *9*, 2308−2315.
(14) Lan, X.; Chen, Z.; Dai, G. L.; Lu, X. X.; Ni, W. H.; Wang, Q. B. Bifacial DNA Origami-Directed Discrete, Three-Dimensional, Anisotropic Plasmonic Nanoarchitectures with Tailored Optical Chirality. *J. Am. Chem. Soc.* **2013**, *135*, 11441−11444.
(15) Tikhomirov, T. DNA-based Programming of Quantum Dot Valency, Self-Assembly and Luminescence. *Nat. Nanotechnol.* **2011**, *6*, 485−490.
(16) Mirkin, C. A.; Letsinger, R. L.; Mucic, R. C.; Storhoff, J. J. A DNA-Based Method for Rationally Assembling Nanoparticles into Macroscopic Materials. *Nature* **1996**, *382*, 607−609.
(17) Maune, H. T. Self-Assembly of Carbon Nanotubes into Two-Dimensional Geometries Using DNA Origami Templates. *Nat. Nanotechnol.* **2010**, *5*, 61−66.
(18) Zhang, H. L.; Chao, J.; Pan, D.; Liu, H. J.; Huang, Q.; Fan, C. H. Folding Super-Sized DNA Origami with Scaffold Strands from Long-Range PCR. *Chem. Commun.* **2012**, *48*, 6405−6407.
(19) Ma, Y. Z.; Zheng, H. N.; Wang, C. E.; Yan, Q.; Chao, J.; Fan, C. H.; Xiao, S. J. RCA Strands as Scaffolds to Create Nanoscale Shapes by A Few Staple Strands. *J. Am. Chem. Soc.* **2013**, *135*, 2959−2962.
(20) Zhao, W.; Ali, M. M.; Brook, M. A.; Li, Y. Rolling Circle Amplification: Applications in Nanotechnology and Biodetection with Functional Nucleic Acids. *Angew. Chem., Int. Ed.* **2008**, *7*, 6330−6337.
(21) Pound, E.; Ashton, J. R.; Becerril, H. C. A.; Woolley, A. T. Polymerase Chain Reaction Based Scaffold Preparation for the Production of Thin, Branched DNA Origami Nanostructures of Arbitrary Sizes. *Nano Lett.* **2009**, *9*, 4302−4305.
(22) Douglas, S. M.; Dietz, H.; Liedl, T.; Hogberg, B.; Graf, F.; Shih, W. M. Self-Assembly of DNA into Nanoscale Three-Dimensional Shapes. *Nature* **2009**, *459*, 414−418.
(23) Zhao, Z.; Yan, H.; Liu, Y. A Route to Scale Up DNA Origami Using DNA Tiles as Folding Staples. *Angew. Chem., Int. Ed.* **2010**, *49*, 1414−1417.
(24) Ke, Y.; Bellot, G.; Voigt, N. V.; Fradkov, E.; Shih, W. M. Two Design Strategies for Enhancement of Multilayer-DNA-Origami Folding: Underwinding for Specific Intercalator Rescue and Staple-Break Positioning. *Chem. Sci.* **2012**, *3*, 2587−2597.
(25) Wen, Y. L.; Pei, H.; Shen, Y.; Xi, J. J.; Lin, M. H.; Lu, N.; Shen, X. Z.; Li, J.; Fan, C. H. DNA Nanostructure-Based Interfacial Engineering for PCR-Free Ultrasensitive Electrochemical Analysis of MicroRNA. *Sci. Rep.* **2012**, *2*, 867.
(26) Wen, Y. L.; Liu, G.; Pei, H.; Li, L. Y.; Xu, Q.; Liang, W.; Li, Y.; Xu, L.; Ren, S. Z.; Fan, C. H. DNA Nanostructure-Based Ultrasensitive Electrochemical MicroRNA Biosensor. *Methods* **2013**, *64*, 276−282.
(27) Pei, H.; Zuo, X. L.; Pan, D.; Shi, J. Y.; Huang, Q.; Fan, C. H. Scaffolded Biosensors with Designed DNA Nanostructures. *NPG Asia Mater.* **2013**, *5*, e51.
(28) Pei, H.; Lu, N.; Wen, Y. L.; Song, S. P.; Liu, Y.; Yan, H.; Fan, C. H. A DNA Nanostructure-Based Biomolecular Probe Carrier Platform for Electrochemical Biosensing. *Adv. Mater.* **2010**, *22*, 4754−4758.
(29) Goodman, R. P.; Schaap, I. A.; Tardin, C. F.; Erben, C. M.; Berry, R. M.; Schmidt, C. F.; Turberfield, A. J. Rapid Chiral Assembly of Rigid DNA Building Blocks for Molecular Nanofabrication. *Science* **2005**, *310*, 1661−1665.
(30) Fakhoury, J. J.; McLaughlin, C. K.; Edwardson, T. W.; Conway, J. W.; Sleiman, H. F. Development and Characterization of Gene Silencing DNA Cages. *Biomacromolecules* **2014**, *15*, 276−282.
(31) de Vries, J. W.; Zhang, F.; Herrmann, A. Drug Delivery Systems Based on Nucleic Acid Nanostructures. *J. Controlled Release* **2013**, *172*, 467−483.
(32) Kim, K.-R.; Kim, D.-R.; Lee, T.; Yhee, J. Y.; Kim, B.-S.; Kwon, I. C.; Ahn, D.-R. Drug Delivery by A Self-Assembled DNA Tetrahedron for Overcoming Drug Resistance in Breast Cancer Cells. *Chem. Commun.* **2013**, *49*, 2010−2012.
(33) Li, J.; Pei, H.; Zhu, B.; Liang, L.; Wei, M.; He, Y.; Chen, N.; Li, D.; Huang, Q.; Fan, C. H. Self-Assembled Multivalent DNA Nanostructures for Noninvasive Intracellular Delivery of Immunostimulatory CpG Oligonucleotides. *ACS Nano* **2011**, *5*, 8783−8789.
(34) Li, J.; Fan, C.; Pei, H.; Shi, J. Y.; Huang, Q. Smart Drug Delivery Nanocarriers with Self-Assembled DNA Nanostructures. *Adv. Mater.* **2013**, *25*, 4386−4396.
(35) Goodman, R. P.; Berry, R. M.; Turberfield, A. J. The Single-Step Synthesis of A DNA Tetrahedron. *Chem. Commun.* **2004**, 1372−1373.
(36) Mastroianni, A. J.; Claridge, S. A.; Alivisatos, A. P. Pyramidal and Chiral Groupings of Gold Nanocrystals Assembled Using DNA Scaffolds. *J. Am. Chem. Soc.* **2009**, *131*, 8455−8459.
(37) Lee, H.; Lytton-Jean, A. K. R.; Chen, Y.; Love, K. T.; Park, A. I.; Karagiannis, E. D.; Sehgal, A.; Querbes, W.; Zurenko, C. S.; Jayaraman, M.; Peng, C. G.; Charisse, K.; Borodovsky, A.; Manoharan, M.; Donahoe, J. S.; Truelove, J.; Nahrendorf, M.; Langer, R.; Anderson, D. G. Molecularly Self-Assembled Nucleic Acid Nanoparticles for Targeted in vivo SiRNA Delivery. *Nat. Nanotechnol.* **2012**, *7*, 389−393.
(38) Erben, C. M.; Goodman, R. P.; Turberfield, A. J. A Self-Assembled DNA Bipyramid. *J. Am. Chem. Soc.* **2007**, *129*, 6992−6993.
(39) Goodman, R. P.; Heilemann, M.; Doose, S.; Erben, C. M.; Kapanidis, A. N.; Turberfield, A. J. Reconfigurable, Braced, Three-Dimensional DNA Nanostructures. *Nat. Nanotechnol.* **2008**, *3*, 93−96.

DOI: 10.1021/am505592e
ACS Appl. Mater. Interfaces 2015, 7, 13174−13179